RSC Advances

ROYAL SOCIETY OF CHEMISTRY

www.rsc.org/advances

Ag Modified AgI-TiO_2 as an Excellent and Durable Catalyst for Catalytic Oxidation of Elemental Mercury

Songjian Zhao, Zan Qu, Naiqiang Yan*, Zhen Li, Wenfei Zhu, Jie pan, Jianfang Xu, Mengdan Li,

AgI-TiO_2 was employed for the removal of elemental mercury (Hg^0) in flue gas, and extra elemental silver (Ag) was introduced to enhance the catalytic activity and stability. AgI-TiO_2 displayed an excellent effect on Hg^0 catalytic oxidation, and the Hg^0 oxidation efficiency was almost 100% with only 5 ppm HCl at 350℃, which was better than that of KI-Ti. Adding Ag to AgI-TiO_2 can prolong the time of high efficiency notably, and the Hg^0 oxidation efficiency was still above 90% after 10 h with only 2% Ag added. Doping with silver could suppress the decomposition of AgI and the loss of iodine, which keep the stability of the catalyst performance. Besides, HCl was readily adsorbed and activated by silver. Iodine in Ag(2%)-AgI-Ti mainly acted as an accelerant for Hg^0 oxidation by facilitating formation of the intermediates Hg-I*, then, chlorine can further convert the intermediate to $HgCl_2$ as the final product.In addition, the thermogravimetric (TG) analysis proved that Ag(2%)-AgI-Ti manifested a good stability at high temperature. Furthermore, the ion chromatograms tests also manifested the chemical stability of AgI-Ti in the presence of Ag.

School of Environmental Science and Engineering, Shanghai Jiao Tong University, 800 Dong Chuan Road, Shanghai, 200240, PR China
* Corresponding author Tel.: +86 21 54745591.
E-mail addresses: nqyan@sjtu.edu.cn

Introduction

The emission of mercury from coal-fired power plants has attracted increasing concern in recent years because of the high toxicity, volatility and bioaccumulation.[1] The Minamata Convention on Mercury, which has been signed by most countries in October 2013, will be put into force to prevent Hg emission worldwide.[2, 3] As one of the largest mercury emission countries, China has also paid increasing attention to mercury control. And the government has issued ‘‘Emission Standard of Air Pollutants for Thermal Power Plants’’ (GB13223-2011) to reduce mercury emissions, which was just implemented in January 2015.[4]

Generally, mercury exists in three forms in coal-fired flue gas: elemental (Hg^0), oxidized (Hg^{2+}), and particle-bound (Hg^p).[5] Hg^{2+} and $Hg(^p)$ are relatively readily to be removed from flue gas by using typical air pollution control devices, such as ESPs and wet-FGD.[6] However, Hg^0 is difficult to be removed from flue gas due to its high volatility and low solubility in water.[7] The technologies for the abatement of Hg^0 mainly focus on two methods: enhanced adsorption or oxidation. The adsorption process, such as halid-modified activated carbon injection, is expensive and may cause secondary environmental problems.[8, 9] Consequently, the catalytic oxidation process is a promising choice, and the generated Hg^{2+} can be subsequently captured by the existing air pollution control devices.

It is reported that HCl is an important specie that affects mercury oxidation, because the major oxidized mercury specie in coal-fired flue gas is $HgCl_2$.[10] Other halogen species could also oxidize Hg^0, such as bromine[11, 12] and iodine, and iodine

was found to be the most efficient oxidant.[13] In addition, HCl would react with HI or I_2 to generate interhalogen specie (ICl), which was a very efficient oxidant for Hg^0 oxidation. [13, 14] However, iodine release might bring unexpected pollution problems if too much iodine was used in flue gas, and I_2 sublimated at a relatively low temperature.

Silver has been recognized as an active catalytic element and subsequently used in various catalysts.[7, 15] Ag was also used as adsorbent materials to remove Hg^0 at low temperatures through an amalgamation mechanism. Besides, Ag can generate electrophilic oxygen, which was beneficial for the reaction. The combination of silver and iodine might enhance the efficiency of Hg^0 oxidation.

In addition, AgI is also a very important catalyst extensively used in photography and photocatalysis field. However, AgI was unstable due to the fact that it would decompose into Ag when exposed to light. Many studies have shown that the metallic silver species existed on the surface were able to inhibit the decomposition of AgX, soadding silver could enhance the catalytic activity and stability.[16, 17] Furthermore, it has found that AgI can maintain its stability when loaded on a semiconductor support such as TiO_2. [18] Therefore, Ag Modified AgI-TiO_2 might be used for catalytic oxidation of elemental mercury. However, no report regarding Ag modified AgI-TiO_2 catalyst for the Hg^0 removal can be acquired as yet.

In the present study, catalysts were prepared using a room-temperature impregnation method. The physical and chemical properties of the catalysts, as well as the Hg^0 oxidation efficiency of the Ag modified AgI-TiO_2 catalyst at low HCl

concentrations, were investigated. Furthermore, the catalytic mechanism involved in improving the efficiency was discussed.

Experimental section

Samples preparation

Catalysts were prepared by the impregnation method, which included KI-TiO_2, AgI-TiO_2, Ag-AgI-TiO_2. For the preparation of KI-TiO_2, an appropriate amount of TiO_2 powder (Degussa P25) and KI were mixed to stir for 1 h, which was marked as A solution, then the A solution was dried with the rotary evaporation apparatus, finally calcined in a muffle furnace (5 h, 500 ℃); For AgI-TiO_2 and Ag-AgI-TiO_2: PVP and $AgNO_3$ precursor were mixed and stirred for 6 h at room temperature, which was added by drops into A solution and stirred constantly for 2 h, then the mixed solution was dried and calcined as above, and the difference between AgI-TiO_2 and Ag-AgI-TiO_2 was that the stoichiometry of Ag.to iodide was more than 1.0 for the latter. The KI-TiO_2, Ag-TiO_2 and Ag-AgI-TiO_2 catalysts are labeled as KI-Ti, Ag-Ti and Ag-AgI-Ti. The element of proportion of the Ag or I to TiO_2 is on the basis of the atom percentages, such as Ag(x%)-Ti represents Ag/TiO_2 mole ratio, and 1% was omitted.

Catalytic Activity Evaluation

The catalytic activity evaluation of the catalysts was similar to that described previously.[7] It consisted of a simulated gas preparation system, catalytic reaction device, a cold vapor atomic absorption spectrometer (CVAAS) and an online data

acquisition system. Hg^0 vapor was prepared from the Hg^0 permeation unit and was blended with the gases before entering the reactor. And the concentration of elemental mercury in the gas was analyzed using a mercury analyzer (CVAAS SG-921). The gas containing the elemental mercury was firstly passed through the bypass and then sent to the CVAAS to determine the baseline. When the concentration of elemental mercury fluctuated within ±5% for more than 30 min, the gas was shifted to the catalytic reactor with catalysts. When the catalyst was saturated by Hg^0, 5 ppm HCl was passed to estimate the Hg^0 oxidation efficiency. Because the catalysts were first saturated in about 300 μg/m^3 of Hg^0 with N_2 and O_2 gas flow, the decrease of Hg^0 concentration across the catalysts after passing HCl was attributed to Hg^0 oxidation. Therefore, the definition of Hg^0 oxidation efficiency (Eoxi) over catalysts is as follows:

$$\text{Eoxi}(\%) = \frac{\Delta Hg^0}{Hg^0_{in}} = \frac{Hg^0_{in} - Hg^0_{out}}{Hg^0_{in}}$$

The gas flow rate was corresponded to a space velocity (SV) of 4.26 × 10^5 h^{-1}. Nitrogen was used as the carrier gas, and the oxygen content was set at 4%.

Characterization of the Catalysts

Powder X-ray diffraction pattern was recorded between 10° and 80° at a step of 7° min^{-1} on an X-ray diffractionmeter (APLX-DUO, BRUKER,Germany) using Cu Ka radiation (40 kv and 20 mA). The microstructure of catalysts was analyzed by transmission electron microscopy (TEM). Samples were dispersed in ethanol with a strong sonication before the analysis. H_2-TPR experiments were performed on Chemisorp TPx 2920 instrument, the catalysts were degassed at 200 ℃ for 3 h under

Ar at atmosphere before H_2-TPR test, the reducing gas was 10% H_2/Ar. The X-ray photoelectron spectroscopy (XPS) measurement was done with an AXIS UItraDLD(Shimadzu-Kratos) spectrometer with Al Ka as the excitation source. The C1s line at 284.8 ev was taken as a reference for the binding energy calibration. The reaction by passing 5000 ppm HCl was monitored in-situ by a UV/vis spectrometer (BDS130, USA) equipped with an optical fiber for UV-beam transmission and a detector in the range of 200-800 nm. The maximum adsorption of UV for iodine, iodine monochloride and chlorine was around at the wavelength of 530 nm, 467 nm and 330 nm, respectively.[19] The reaction product were dissolved into the ultrapure water and analyzed by ion chromatography (BP-100). The thermal stability of catalysts was performed by the TGA/DSC1 (Mettler Toledo), N_2 was as carrier gas, and the heating rate was 5 ℃/min. Hg^0 adsorption experiment was conducted by passing flue gas contained Hg^0, N_2 and 4% O_2 into prepared catalyst, and recording the Hg^0 signal curve. The temperature programmed desorption(TPD) curves of Hg^0 proceeded as follows: an appropriate amount of catalyst was placed in fixed-bed reactor with N_2 + 4% O_2 at 30 L/h and 100 ℃ to adsorb mercury for 2 h; afterwards, the oxygen was stopped, and the Hg^0 signal curve was recorded at 2 ℃/min until 450 ℃ under nitrogen.

Results and discussion

Comparison of the Hg^0 catalytic oxidation efficiencies of various catalysts

Figure 1

Figure 1 shows the comparison of the Hg^0 catalytic oxidation efficiencies over various catalysts at 350 ℃. The Hg^0 oxidation efficiency of AgI-Ti was higher than that of KI-Ti, which indicated that there were more active species to oxidize Hg^0 after HCl was passed for AgI-Ti. While the Hg^0 oxidation efficiency was reduced with time, suggested that the performance of AgI-Ti was unstable. When silver was added, the high efficiency time was obviously prolonged. However, the efficiency was declined for high silver content, which might be that high content of silver inhibited the catalysis of AgI. And 2% Ag content was suitable. The Hg^0 oxidation efficiency was still above 90% after 10 h, indicated that Ag(2%)-AgI-Ti was a high-performance catalyst for the Hg^0 catalytic oxidation. Besides, the Hg^0 catalytic performance of Ag(1%)-AgI-Ti was better than that of Ag(1%)-AgCl-Ti and Ag(1%)-AgBr-Ti, manifested that iodine was the most efficient for Hg^0 oxidation among halogen species. Therefore, the physical and chemical properties of the catalysts and the reaction mechanism were necessary to study.

Catalysts activity

Figure 2

Figure 2 shows the Hg^0 oxidation efficiencies over Ag(2%)-AgI-Ti at various temperatures after passing 5 ppm HCl. As can be seen from Figure 2, the catalytic

efficiency of Ag(2%)-AgI-Ti was improved with the increase of temperature, and the Hg^0 oxidation efficiency could reach 100% above 350 ℃. It indicated that the suitable reaction temperature for oxidizing Hg^0 was at high temperature, and there were more active species to oxidize Hg^0 at high temperature.

Figure 3

The Hg^0 catalytic oxidation efficiencies of Ag(2%)-AgI-Ti with various cases are showed in Figure 3. Ag(2%)-AgI-Ti had little catalytic ability in the condition of only O_2 or HCl. And when O_2 and HCl coexisted, the oxidation efficiency was high, manifested that HCl was the mainly catalytic component. Active Cl or Cl_2 would be generated by the catalysis of Ag(2%)-AgI-Ti with the presence of O_2, which could react with AgI to produce ICl or I_2 to oxidize Hg^0. When 500 ppm SO_2 was passed, the performance of catalyst was slightly inhibited, which might be that some of active Cl would react with SO_2.[13] And the efficiency improved slightly when adding 500 ppm NO, indicated NO promoted the Hg^0 oxidation.[20] In addition, 4% H_2O was little effect on the Hg^0 oxidation.

Microstructural characterizations

Figure 4

Table 1

To obtain the microscopic morphologies information, transmission electron microscopy (TEM) analyses of the AgI-Ti and Ag(2%)-AgI-Ti nanoparticles were carried out, as shown in Figure 4. The AgI-Ti catalyst was nanoparticles and the sizes were between 20 and 40 nm from Figure 4 (a). The element content of AgI-Ti by the EDS analysis in table 1 could prove the existence of AgI on the carrier. Besides, the HRTEM image in Figure 4 (b) corresponding to the circled in Figure 4 (a) shows the crystal lattices with distances of 0.23 nm and 0.35 nm, which can be attributed to the (110) plane of β-AgI and the (1 0 1) plane of anatase TiO_2, respectively, to further prove the existence of AgI on the TiO_2.[21 22] There were many small particles attached on the surfaces of TiO_2 in Figure 4 (c), which was Ag nanoparticles compared with Figure 4 (a). And the AgI nanoparticles were also found by HRTEM image in Figure 4 (d) corresponding to the circled in Figure 4 (c). Besides, the content of idoine for Ag-(2%)-AgI-Ti was higher than that of AgI-Ti according to the result of table 1. It indicated that the catalyst was prepared successfully and adding the silver could inhibit the decomposition of AgI efficiently.

X-ray diffraction study

Figure 5

Figure 5 shows the XRD patterns of the various catalysts calcined at 500 ℃. The anatase and the rutile phases of TiO_2 can be seen for all catalysts in Figure 5. The peak at 32.8 ev was indexed to (1 0 2) planes of the hexagonal β-AgI crystal phase [16],

198 which was weak in Figure 5 (b-d) due to the low content. Additionally, no noticeable
199 silver oxide and metal peaks were observed in the X-ray diffractograms in Figure 5 (b)
200 and (c), because the amount of Ag dopant was low or the strongest Ag peak (1 1 1)
201 was overlapped with that of anatase (0 0 4). The Ag^0 characteristic peaks could be
202 observed in Figure 5 (d), indicated that additive silver was loaded on the support in
203 the form of metallic state.

204

205 **XPS analysis**

206

207 **Figure 6**

208

209 Figure 6 shows the XPS spectra of AgI-Ti and Ag(2%)-AgI-Ti over the spectral
210 regions of Ag 3d, I 3d, O 1s, Ti 2p, Cl 2p and Hg 2p. The spectra of I 3d in Figure 6 (a)
211 shows that the binding energies of I 3d5/2 and I 3d3/2 were locatedat about 630.5 eV
212 and 618.5 eV, respectively, which could be ascribed to the I^- in AgI.[23, 24] The I 3d
213 peaks of Ag(2%)-AgI-Ti were enhanced compared with that of AgI-Ti, suggested that
214 the content of iodine was higher for Ag(2%)-AgI-Ti. It indicated that the addition of
215 silver could maintain the stability of AgI and was beneficial for the catalytic reaction.
216 After passing HCl, the strength of I 3d peaks was weakened, which might be that Hg^0
217 or Cl species was adsorbed on the surface of iodine.

218 Figure 6 (b) shows the XPS peaks of Ag 3d. It was reported that the peaks at
219 367.90 eV and 373.94 eV were attributed to Ag (I), and those at 368.23 eV and 374.09

eV were attributed to metallic silver Ag (0).[21] It could find that the silver nanoparticles were present in a mixture of metallic silver (Ag^0) and Ag^+ (AgI) for AgI-Ti and Ag(2%)-AgI-Ti, in which the Ag^+ was dominant, manifested the existence of AgI, and it could also conclude that some of AgI was decomposed to Ag^0. By adding silver to AgI-Ti, the more content of metallic silver could stabilize AgI, so that the Ag^+ peak intensity of Ag(2%)-AgI-Ti was increased. After passing HCl, the intensity of the characteristic peaks was weakened. It might because HCl or Cl was adsorbed on the surface of Ag. The characteristic peak of silver was shifted to low binding energy due to the effect of HCl.

The O 1s XPS spectrum is shown in Figure 6 (c). The peak at 529.8 eV might be ascribed to lattice oxygen, and the peak at 531.4 eV could be attributed to surface chemisorbed oxygen. Besides, the peak at 528.2 eV was nucleophilic states and 530.4 eV denoted electrophilic states for the O 1s, and the electrophilic oxygen was beneficial for oxidation reaction. [7] It could be found from Figure 6 (c) that there was no nucleophilic oxygen after adding silver, and the chemisorbed oxygen and electrophilic oxygen existed, which was beneficial for the oxidation ability of catalyst. And when the HCl was passed, the surface chemisorbed oxygen was decreased, suggested that HCl and oxygen were activated by silver and reacted with each other. The reaction path might be that the electron of HCl transferred by silver to the chemisorbed oxygen. Active chlorine was produced and then oxidized I^- or Hg^0, and generated oxygen anion combined with hydrogen ions into water.[17]

The two typical Ti 2p peaks located at approximately 458.56 eV and 464.24 eV

can be assigned to Ti^{4+} 2p3/2 and Ti^{4+} 2p1/2, respectively in Figure 6 (d).[25] An additional peak at 457 eV for AgI-Ti in Figure 6 (d) was detected that matched the trivalent state of titanium,[25] which was disappeared for Ag(2%)-AgI-Ti. And an obvious shoulder at about 460.4 ev was also attributed to Ti^{4+} 2p3/2, [26] shown in Figure 6 (d). It indicated that the surface-deposited Ag could induce a change in the Ti chemical states, maintaining the higher oxidation states of Ti.

The Cl 2p XPS spectrum is shown in Figure 6 (e). There were two peaks at 197.8 and 199.7 eV for Cl 2p, which were attributable to ionic (Cl^-) and covalent (– Cl) chlorine species, respectively.[27] The ionic chlorine (Cl^-) might be the $HgCl_2$ generated by the reaction of chlorine species and mercury or chlorine species and HgI_2.[19] And the covalent (– Cl) chlorine species might the adsorbed HCl or generated ICl.

The Hg 4f XPS patterns are shown in Figure 6 (f). As can be found the peak of Hg 4f was at about 101.8 eV, which was significantly higher than the binding energy of Hg^0 (99.9 eV).[28] It inferred that there was no Hg^0 on the surface of catalyst. Tao, et al. reported that the binding energies for Hg 4f 5/2 and Hg 4f 7/2 can be attributed to HgO (with the peak at 104.4 eV) and $HgCl_2$ (101.4 eV).[29] The Hg 4f peak in Figure 6 (f) could be Hg^{2+}, indicated that Hg^0 was oxidized by the catalyst. Besides, the Hg 4f was weak, which was suggested that the reaction production was adsorbed less on the surface of catalyst, and most of mercury oxidation was in the gas.

TPR analysis

Figure 7

The TPR profiles of the various catalysts are shown in Figure 7. As can be seen in the Figure 7, p25 was no obvious peak, and the oxidation ability was weak. There was a peak at about 600 ℃ for KI-Ti, showed that catalyst started to decompose to form I_2 under this temperature. In addition, it can be seen clearly that the oxidation ability of AgI-Ti and Ag(2%)-AgI-Ti was higher than that of KI-Ti and the catalytic performance was stable. And the peak at 180 ℃ was stronger for Ag(2%)-AgI-Ti, which might be due to the larger proportion of Ag^0, easier to produce active hydrogen and hydrogen overflow or Ag_2O.[30] As can be also seen that the performance of Ag(2%)-AgI-Ti was more stable with the increase of temperature than that of AgI-Ti, indicated the important role of silver.

The analysis of the catalytic mechanism

The analysis of the mercury combination property

Figure 8

In order to study the mercury combination property of catalysts, the Hg^0 adsorption and desorption experiments were performed. Figure 8 (a) shows the Hg^0 breakthrough curves over Ag(2%)-AgI-Ti at various temperatures. As can be seen from Figure 8 (a), the adsorption ability of Hg^0 was poor above 300 ℃, indicated that Hg^0 was hardly adsorbed at high temperature. Besides, AgI was stable and not

decomposed below 400 ℃. While the Hg^0 concentration was reduced slightly at 450 ℃, it might be the generated active I, which oxidized Hg^0. And the Hg^0 concentration still high, indicated the amount of active I was less and AgI was still stable.

The Hg-TPD curves for Ag(2%)-AgI-Ti are shown in Figure 8 (b). It can be seen from Figure 8 (b), some amount of Hg^0 was desorbed at low temperature, which might be the decomposition of the silver amalgam. And there were little desorbed Hg^0 above 300 ℃, indicated that Hg^0 was hardly adsorbed on the surface of catalyst at high temperature in accordance with the results of Figure 8 (a). The Hg^0 concentration reduced at 450 ℃, which might be the small amounts of active I was generated.

The analysis of UV/vis spectrum

Figure 9

In order to probe on the role of HCl for Hg^0 oxidation, the reaction by passing HCl over Ag(2%)-AgI-Ti was recorded by the UV/vis spectrometer. There were no obvious characteristic peaks for Ag(2%)-AgI-Ti until the concentration of HCl was 5000 ppm, and the results were shown in Figure 9. Figure 9 (a) shows the comparison of the UV/vis spectrum of various catalysts at 5000 ppm HCl. There was no characteristic peak for KI-Ti, while an absorption peak of 530 nm can be seen for AgI-Ti and Ag(2%)-AgI-Ti in Figure 9 (a), which was attributed to I_2. This result suggested that the iodine was formed by adding HCl, and Ag might have a catalytic

effect for HCl. Active chlorine could be generated and then oxidized iodine ion to active iodine. And due to the high concentration of HCl, the amount of active iodine would be more, so that the reaction was strong to generate I_2. The peak of I_2 of Ag(2%)-AgI-Ti was stronger than that of AgI-Ti, which might be due to relatively high iodine content, indicated that more silver nanoparticles could inhibit the decomposition of AgI.

The UV/vis spectrum of Ag(2%)-AgI-Ti at different temperatures were shown in Figure 9 (b). The absorption peak intensity at 530 nm (I_2) increased with the increasing temperature, suggested that the yield of I_2 increased with increasing temperature. The number of active Cl might increase with temperature rise, so that the more amount of active I were generated, meant that Hg^0 would be oxidized more effectively over catalyst at high temperature.

The analysis of ion chromatograms

Figure 10

To determine reaction products, ion chromatography analysis was employed to analyze the oxidized mercury products, which were dissolved into the ultrapure water. Figure 10 shows the ion chromatograms of reaction product. It can be seen from Figure 10 (b) that there was only one characteristic peak, which can be attributed to Cl^-, compared the peak of the standard sample in Figure 10 (a). It was reported iodine was more reactive than chlorine (two magnitudes) for the removal of Hg^0,[19] while the

peak of I^- was not found, indicted that the reaction product was not HgI_2. It may be that active I combined with Hg^0 in the formation of van der Waals intermediate molecules, such as Hg-I*, and then active chlorine converted the intermediate to $HgCl_2$, which was because chlorine was more competitive than iodine to bond with the oxidized mercury due to the higher redox potential value.[32] Besides, active I would react with silver to generate AgI, maintaining the stability of iodine.

Base on the above results, the possible reaction paths for Hg^0 removal could be speculated as follows: HCl was adsorbed and activated by silver nanoparticles, and the generated Cl activated AgI to Ag···I*. Then Ag···I* combined with Hg^0 in the form of Hg-I*, which reacted with adsorbed Cl on the surface of silver to generate $HgCl_2$ and AgI, maintained the stability of Ag(2%)-AgI-Ti catalyst.

Figure 11

The main reaction process for the Hg^0 oxidation over Ag(2%)-AgI-Ti can be showed in the Figure 11. As can be seen from Figure 11, iodine in Ag(2%)-AgI-Ti mainly acted as an accelerant for Hg^0 oxidation by facilitating formation of the intermediates. And then chlorine can further convert the intermediate to the final product of $HgCl_2$. AgI was recycled in the reaction process, which was beneficial for the Hg^0 oxidation at a long time.

Eqs. (1)–(5) are some of the possible reactions during Hg^0 conversion:

$$4Ag\cdots HCl + O_2 \rightarrow 4Ag\cdots Cl^* + 2H_2O \quad (1)$$

$$AgI + Ag\cdots Cl^{*} \rightarrow Ag\cdots I^{*} + Ag\cdots Cl \quad (2)$$

$$Ag\cdots I^{*} + Hg^{0} \rightarrow Ag + Hg\cdots I^{*} \quad (3)$$

$$Hg\cdots I^{*} + Ag\cdots Cl \rightarrow HgCl + AgI \quad (4)$$

$$HgCl + Cl^{*} \rightarrow HgCl_{2} \quad (5)$$

The analysis of thermal stability

Figure 12

In order to study the thermal stability of catalysts, the thermogravimetric (TG) analysis was performed. Figure 12 shows the TG curves of various catalysts. As can be seen from the Figure 12, the weights of AgI-Ti and Ag (2%)-AgI-Ti were declined below 300 ℃, which might be the surface adsorption of water. And the weight of AgI-Ti was still declined slowly above 300 ℃, indicated that some of AgI might be decomposed to I_2 at high temperature. While the weight of Ag (2%)-AgI-Ti was reduced little, manifested a very good stability at high temperature, and proved that Ag could inhibit the decomposition of AgI efficiently.

Figure 13

To verify the chemical stability of iodide, ion chromatography analysis was used to detect the amount change of iodide. The experiment process was as follows: a certain amount of Ag (2%)-AgI-Ti catalyst reacting for 10 h and fresh catalyst were

dissolved in sodium thiosulfate solution by ultrasonic dispersion for 24 h, and then the supernatant of mixture was analyzed. Figure 13 recorded the ion chromatograms of Ag (2%)-AgI-Ti before and after reaction. The characteristic peak of iodine can be found in Figure 13 (a) and (b), manifested that iodine still existed on the surface of catalyst. It revealed the stability of iodine, and proved the conclusion above, which iodine was accelerant for Hg^0 oxidation by facilitating formation of the intermediates. However, the amount of iodine was decreased slightly, and the loss amount was about 20% for 10 h, which might be that the active I on the surface of catalyst was take away due to the higher space velocity. At actual condition, space velocity could be adjusted to reduce the loss of iodine, and iodine vapour could be also passed to catalyst to recover the iodine amount. Furthermore, the characteristic peak of chlorine was seen in Figure 13. The peak intensity after reaction was stronger than that of catalyst before reaction to prove that chlorine was adsorbed on the surface of catalyst.

Conclusions

Ag(2%)-AgI-TiO_2 was an excellent and durable catalyst for Hg^0 catalytic oxidation, and can reach 100% with 5 ppm HCl at 350 ℃, which was better than KI-Ti. Adding silver to AgI-TiO_2 can prolong effectively the time of high efficiency. And 2% Ag content was suitable, for which the Hg^0 oxidation efficiency was still above 90% after 10 h. AgI and Ag nanoparticles were loaded on the surface of TiO_2, and the addition of silver could inhibit the decomposition of AgI by the analysis of physical and chemical characterization. The component analysis of Hg^0 oxidation indicated that HCl was the major oxidation component and O_2 was necessary, besides,

sulfur dioxide inhibited slightly the Hg^0 oxidization, while nitric oxide can promote the reaction, and water had little effect on the reaction. The reaction mechanism was probed by UV/vis spectrums ion chromatography analysis, indicated that HCl was adsorbed and activated by silver, and the generated Cl activated AgI to Ag···I*. Then Ag···I* combined with Hg^0 in the form of Hg-I*, which reacted with adsorbed Cl on the surface of silver to generate $HgCl_2$ and AgI, maintained the stability of Ag(2%)-AgI-Ti catalyst. In addition, the thermogravimetric (TG) analysis was performed, proved that Ag (2%)-AgI-Ti manifested a good stability at high temperature. Furthermore, the ion chromatograms of Ag (2%)-AgI-Ti before and after the reaction revealed the chemical stability of AgI-Ti in the presence of Ag.

Acknowledgements

This study was supported by the Major State Basic Research Development Program of China (973 Program, No.2013CB430005), the National Natural Science Foundation of China (No.50908145) and the National High-Tech R&D Program (863) of China (No.2011AA060801).

References

1. Y. Zhao, R. L. Hao, P. Zhang and S. H. Zhou, *Fuel*, 2014, 136, 113-121.
2. A. Suarez Negreira and J. Wilcox, *Energy & Fuels*, 2014.
3. S. S. Chen, H. C. Hsi, S. H. Nian and C. H. Chiu, *Applied Catalysis B-Environmental*, 2014, 160, 558-565.
4. J. K. Xie, Z. Qu, N. Q. Yan, S. J. Yang, W. M. Chen, L. G. Hu, W. J. Huang and P. Liu, *Journal of Hazardous Materials*, 2013, 261, 206-213.
5. H. Q. Yang, Z. H. Xu, M. H. Fan, A. E. Bland and R. R. Judkins, *Journal of Hazardous Materials*, 2007, 146, 1-11.
6. A. Beretta, N. Usberti, L. Lietti, P. Forzatti, M. Di Blasi, A. Morandi and C. La Marca, *Chemical*

Engineering Journal, 2014, 257, 170-183.
7. S. J. Zhao, Y. P. Ma, Z. Qu, N. Q. Yan, Z. Li, J. K. Xie and W. M. Chen, *Catalysis Science & Technology*, 2014, 4, 4036-4044.
8. S. Aboud, E. Sasmaz and J. Wilcox, *Main Group Chemistry*, 2008, 7, 205-215.
9. F. Scala, *Environmental Science & Technology*, 2001, 35, 4367-4372.
10. A. A. Presto and E. J. Granite, *Environmental Science & Technology*, 2006, 40, 5601-5609.
11. E. Sasmaz, A. Kirchofer, A. D. Jew, A. Saha, D. Abram, T. F. Jaramillo and J. Wilcox, *Fuel*, 2012, 99, 188-196.
12. J. Wilcox, E. Sasmaz, A. Kirchofer and S.-S. Lee, *Journal of the Air & Waste Management Association*, 2011, 61, 418-426.
13. Y. Chi, N. Q. Yan, Z. Qu, S. H. Qiao and J. P. Jia, *Journal of Hazardous Materials*, 2009, 166, 776-781.
14. S. H. Liu, N. Q. Yan, Z. R. Liu, Z. Qu, P. Wang, S. G. Chang and C. Miller, *Environmental Science & Technology*, 2007, 41, 1405-1412.
15. Y. H. Yeom, M. J. Li, W. M. H. Sachtler and E. Weitz, *Journal of Catalysis*, 2007, 246, 413-427.
16. H. Xu, J. Yan, Y. G. Xu, Y. H. Song, H. M. Li, J. X. Xia, C. J. Huang and H. L. Wan, *Applied Catalysis B-Environmental*, 2013, 129, 182-193.
17. H. X. Shi, G. Y. Li, H. W. Sun, T. C. An, H. J. Zhao and P. K. Wong, *Applied Catalysis B-Environmental*, 2014, 158, 301-307.
18. C. Hu, X. X. Hu, L. S. Wang, J. H. Qu and A. M. Wang, *Environmental Science & Technology*, 2006, 40, 7903-7907.
19. Z. Qu, N. Yan, P. Liu, J. Jia and S. Yang, *Journal of hazardous materials*, 2010, 183, 132-137.
20. N. Q. Yan, W. M. Chen, J. Chen, Z. Qu, Y. F. Guo, S. J. Yang and J. P. Jia, *Environmental Science & Technology*, 2011, 45, 5725-5730.
21. Y. H. Zhang, Z. R. Tang, X. Z. Fu and Y. J. Xu, *Applied Catalysis B-Environmental*, 2011, 106, 445-452.
22. W. Sun, Y. Z. Li, W. Q. Shi, X. J. Zhao and P. F. Fang, *Journal of Materials Chemistry*, 2011, 21, 9263-9270.
23. L. Dong, Y. He, T. Li, J. Cai, W. Hu, S. Wang, H. Lin, M. Luo, X. Yi, L. Zhao, W. Weng and H. Wan, *Applied Catalysis a-General*, 2014, 472, 143-151.
24. J. Cao, Y. Zhao, H. Lin, B. Xu and S. Chen, *Journal of Solid State Chemistry*, 2013, 206, 38-44.
25. S. B. Atla, C.-C. Chen, C.-Y. Chen, P.-Y. Lin, W. Pan, K.-C. Cheng, Y. M. Huang, Y.-F. Chang and J.-S. Jean, *Journal of Photochemistry and Photobiology a-Chemistry*, 2012, 236, 1-8.
26. C. F. Almeida Alves, F. Oliveira, I. Carvalho, A. P. Piedade and S. Carvalho, *Materials Science & Engineering C-Materials for Biological Applications*, 2014, 34, 22-28.
27. P. M. Carrasco, M. Cortazar, E. Ochoteco, E. Calahorra and J. A. Pomposo, *Surface and Interface Analysis*, 2007, 39, 26-32.
28. M. Bentley, M. Fan, B. Dutcher, M. Tang, M. D. Argyle, A. G. Russell, Y. Zhang, M. P. Sharma and S. M. Swapp, *Journal of Hazardous Materials*, 2013, 262, 642-648.
29. S. Tao, C. Li, X. Fan, G. Zeng, P. Lu, X. Zhang, Q. Wen, W. Zhao, D. Luo and C. Fan, *Chemical Engineering Journal*, 2012, 210, 547-556.
30. X. Ge and H.-l. Zhang, *Journal of Solid State Chemistry*, 1998, 141, 186-190.
31. S. Zhao, Y. Ma, Z. Qu, N. Yan, Z. Li, J. Xie and W. Chen, *Catalysis Science & Technology*, 2014, 4, 4036-4044.

32. Z. Qu, N. Q. Yan, P. Liu, Y. P. Chi and J. Jia, *Environmental Science & Technology*, 2009, 43, 8610-8615.

Table/ Figure Captions

Table 1. The element content of AgI-Ti and Ag(2%)-AgI-Ti by the EDS analysis

Figure 1. The comparison of the Hg^0 catalytic oxidation efficiencies over various catalysts at 350 ℃

Figure 2. The Hg^0 oxidation efficiencies over Ag(2%)-AgI-Ti at various temperatures after passing 5 ppm HCl

Figure 3. The Hg^0 catalytic oxidation efficiencies of Ag(2%)-AgI-Ti with various cases

Figure 4. TEM and HRTEM images: AgI-Ti (a, b) and Ag (2%)-AgI-Ti (c, d)

Figure 5. The XRD patterns of the various catalysts calcined at 500 ℃

Figure 6. The XPS spectra of AgI-Ti and Ag(2%)-AgI-Ti over the spectral regions: I 3d (a), Ag 3d (b), O 1s (c), Ti 2p (d), Cl 2p (e) and Hg 2p (f)

Figure 7. TPR profiles of the various catalysts: P25 (a), KI-Ti (b), AgI-Ti (c), Ag(2%)-AgI-Ti (d)

Figure 8. The Hg^0 adsorption and desorption curves over Ag(2%)-AgI-Ti: The Hg^0 breakthrough curves at various temperatures (a), The Hg-TPD curves (b)

Figure 9. The UV/vis spectrum analysis: The comparison of various catalysts (a), Ag(2%)-AgI-Ti at different temperatures (b)

491 **Figure 10. The ion chromatograms of reaction product**

492 **Figure 11. The main reaction process for the Hg^0 oxidation over Ag (2%)-AgI-Ti**

493 **Figure 12. The TG curves of various catalysts: AgI-Ti (a), Ag (2%)-AgI-Ti (b)**

494 **Figure 13. The ion chromatograms of Ag (2%)-AgI-Ti before and after the reaction**

495

Table 1

Table 1 The element content of AgI-Ti and Ag(2%)-AgI-Ti by the EDS analysis

	Element	Weight%	Atomic%
Ag(2%)-AgI-Ti	O K	44.69	71.96
	Ti K	49.77	26.77
	Ag L	4.27	1.02
	I L	1.26	0.26
AgI-Ti	O K	83.36	94.24
	Ti K	14.17	5.35
	Ag L	2.08	0.35
	I L	0.39	0.06
	Totals	100.00	

Figure 1

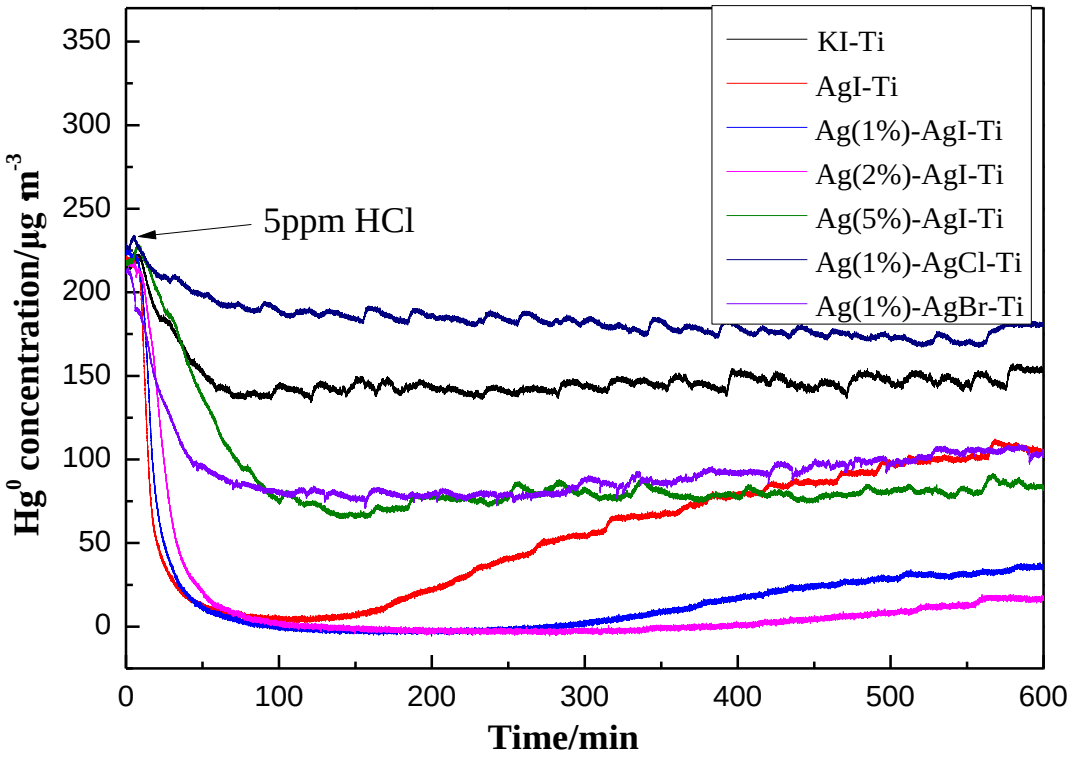

508 **Figure 2**

509

510

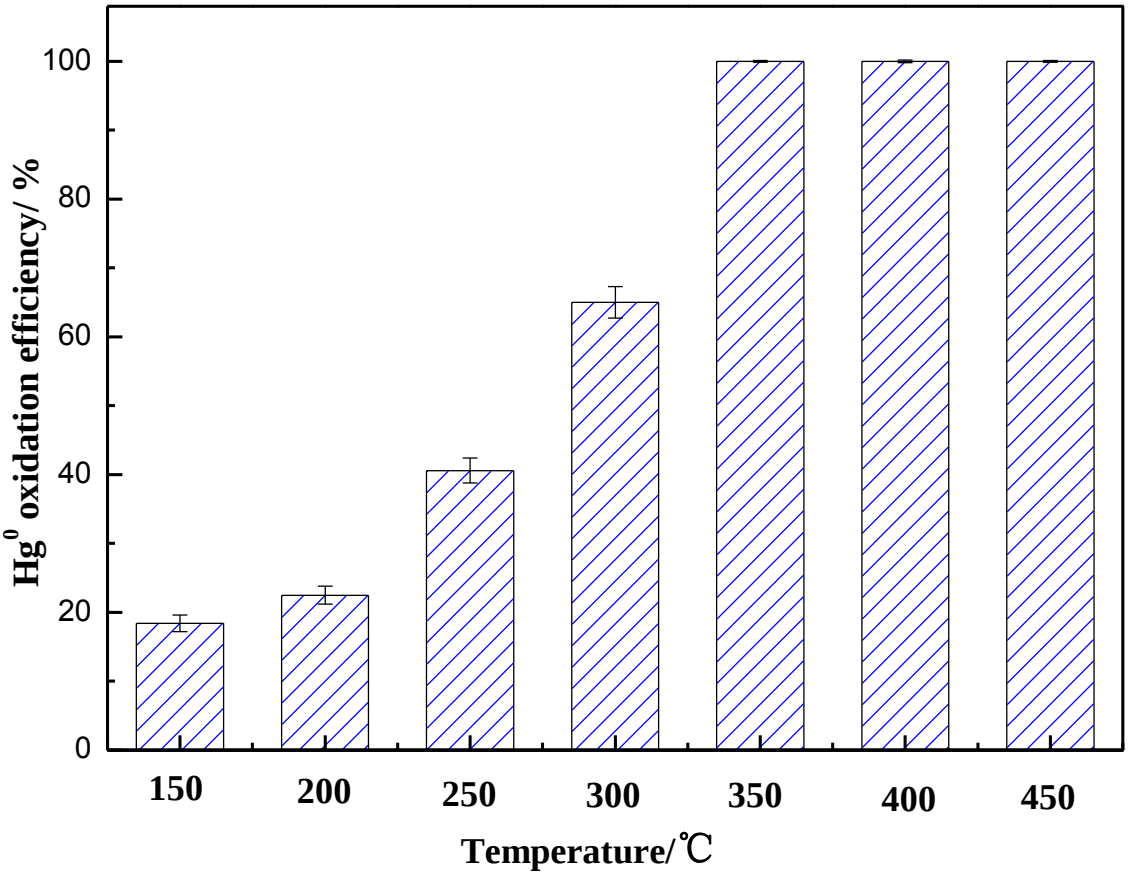

511

512

513

514 **Figure 3**

515

516

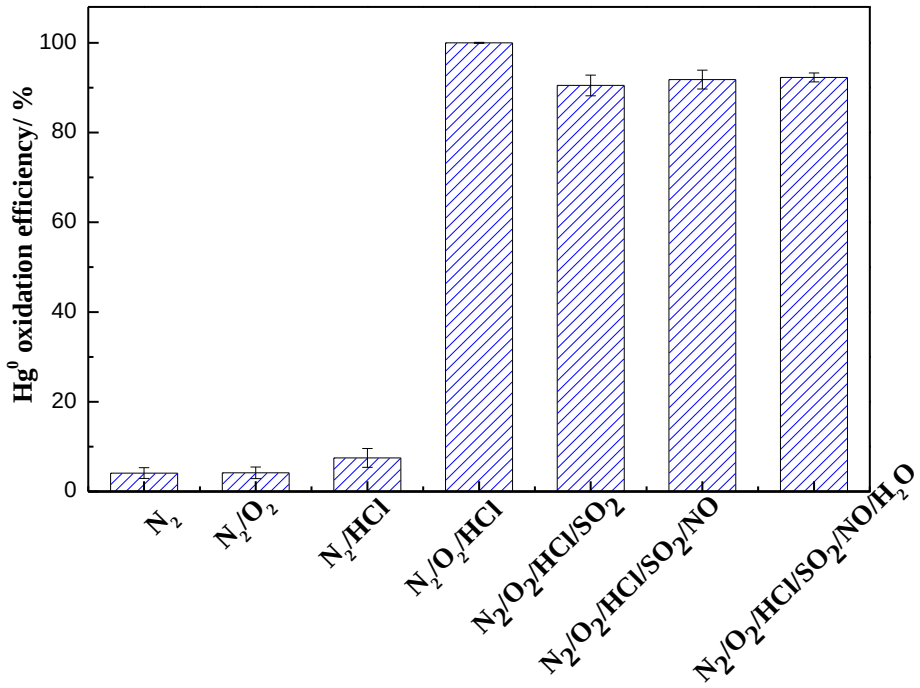

517

518

519

Figure 4

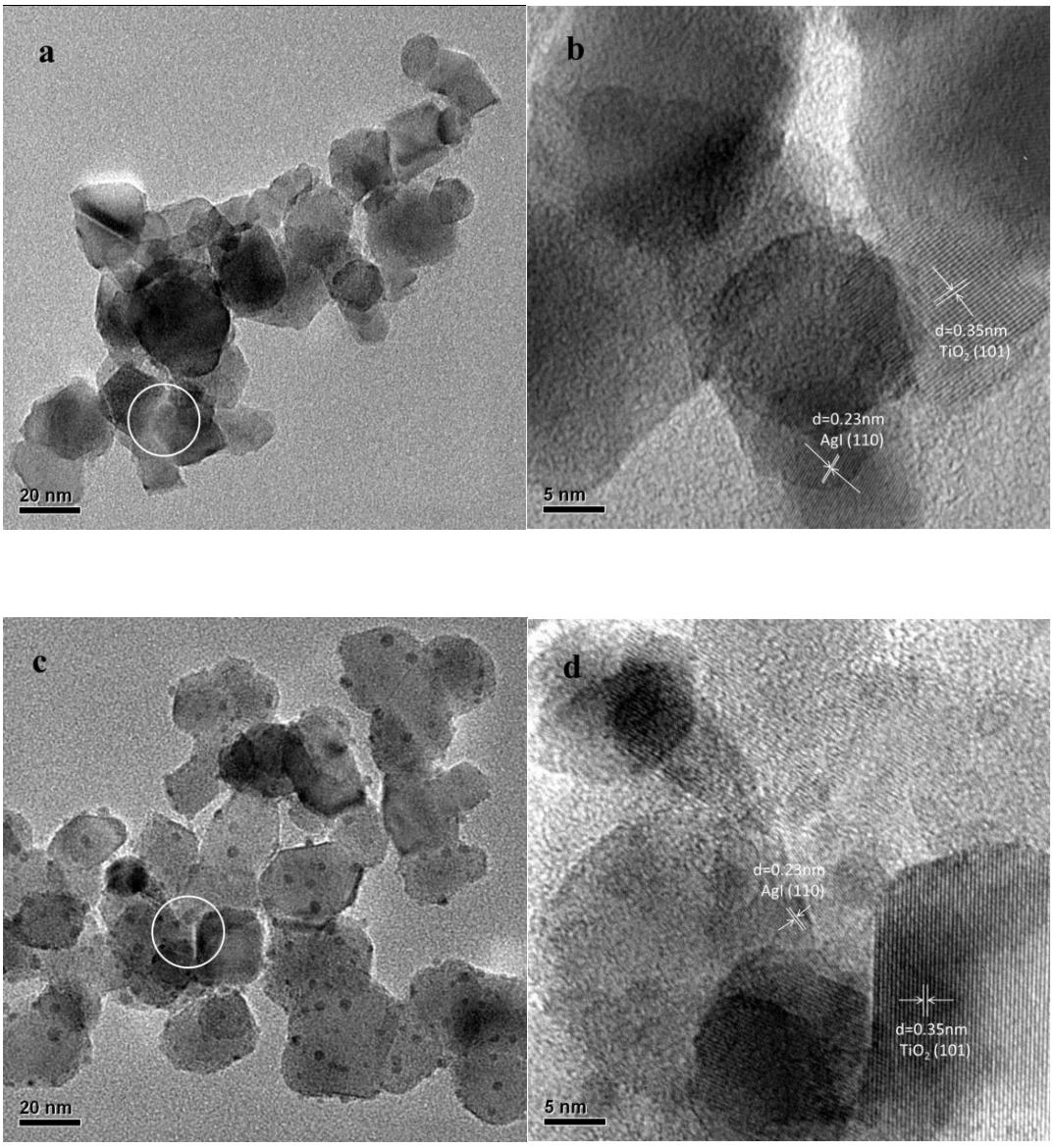

528 **Figure 5**

529

530

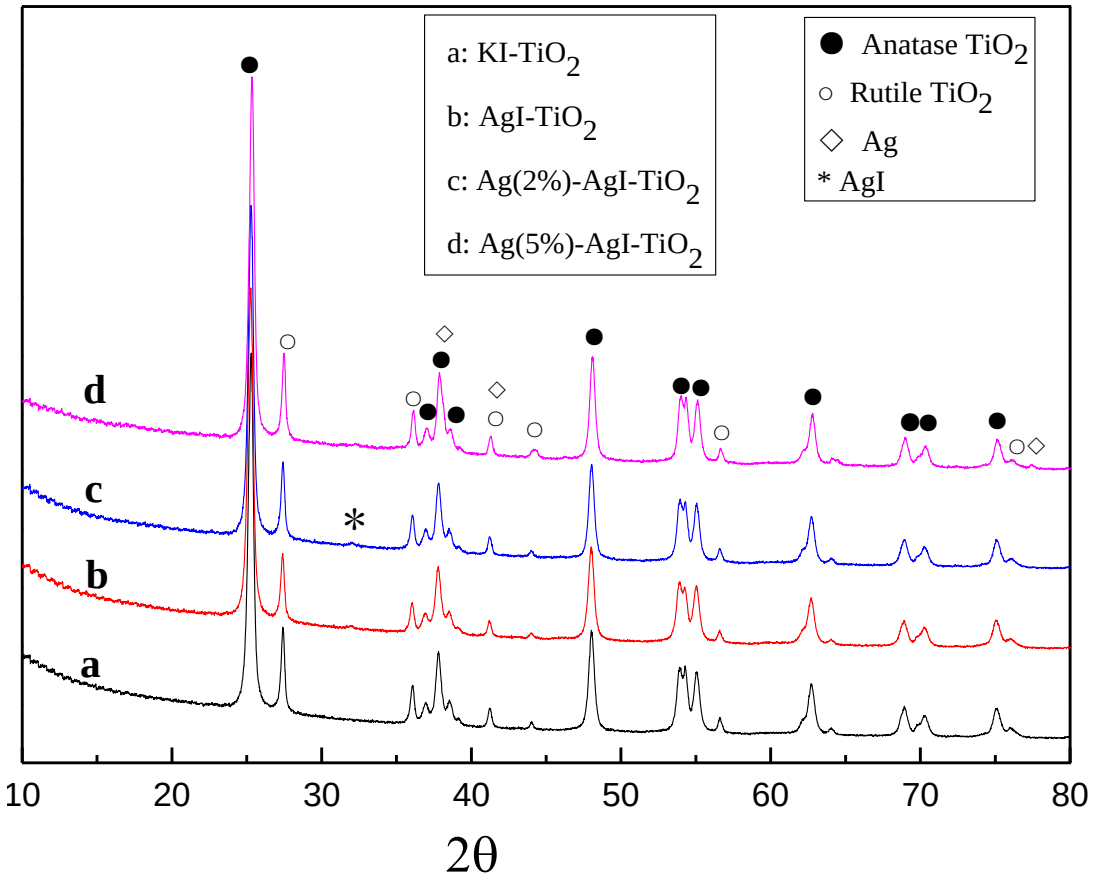

531

532

Figure 6

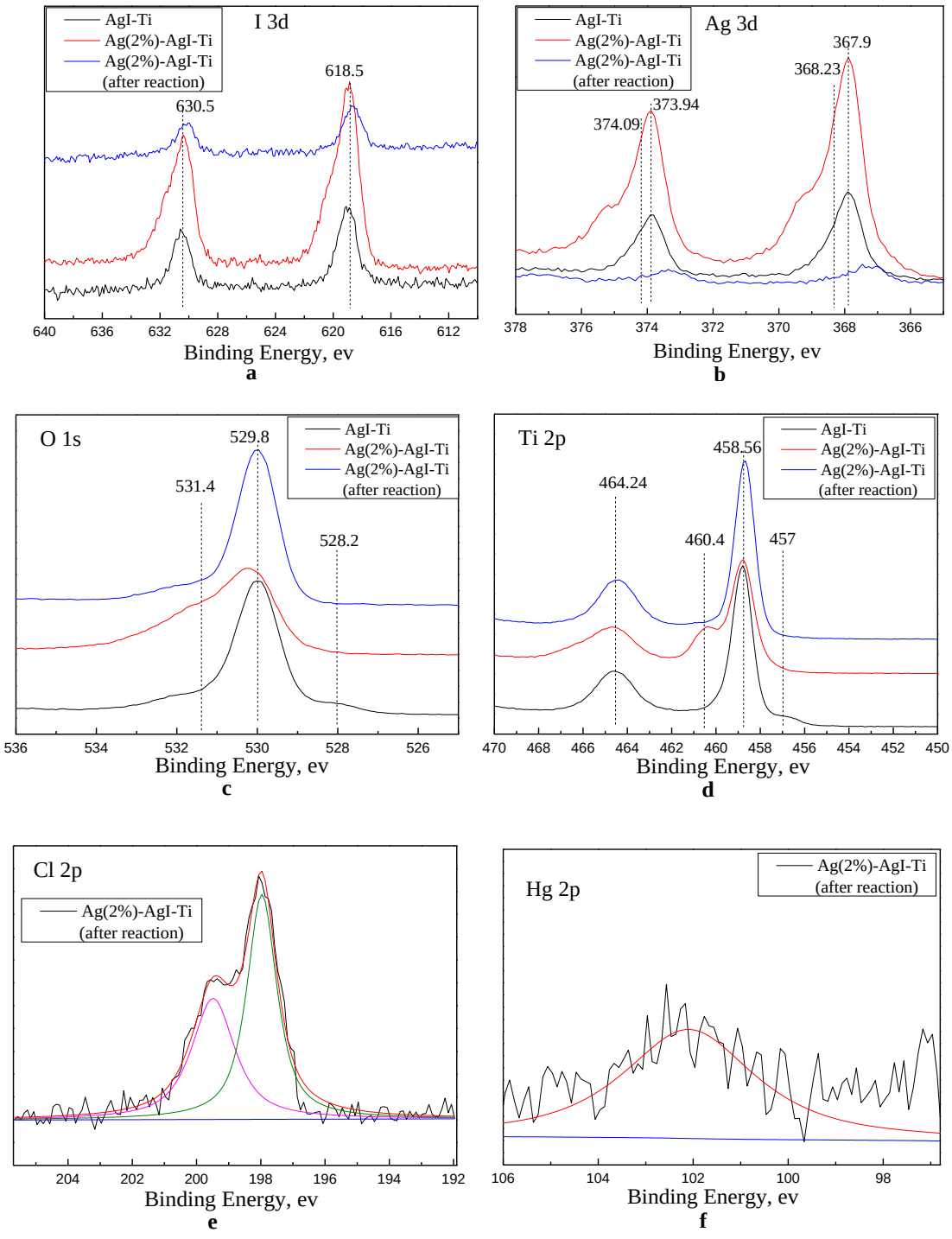

Figure 7

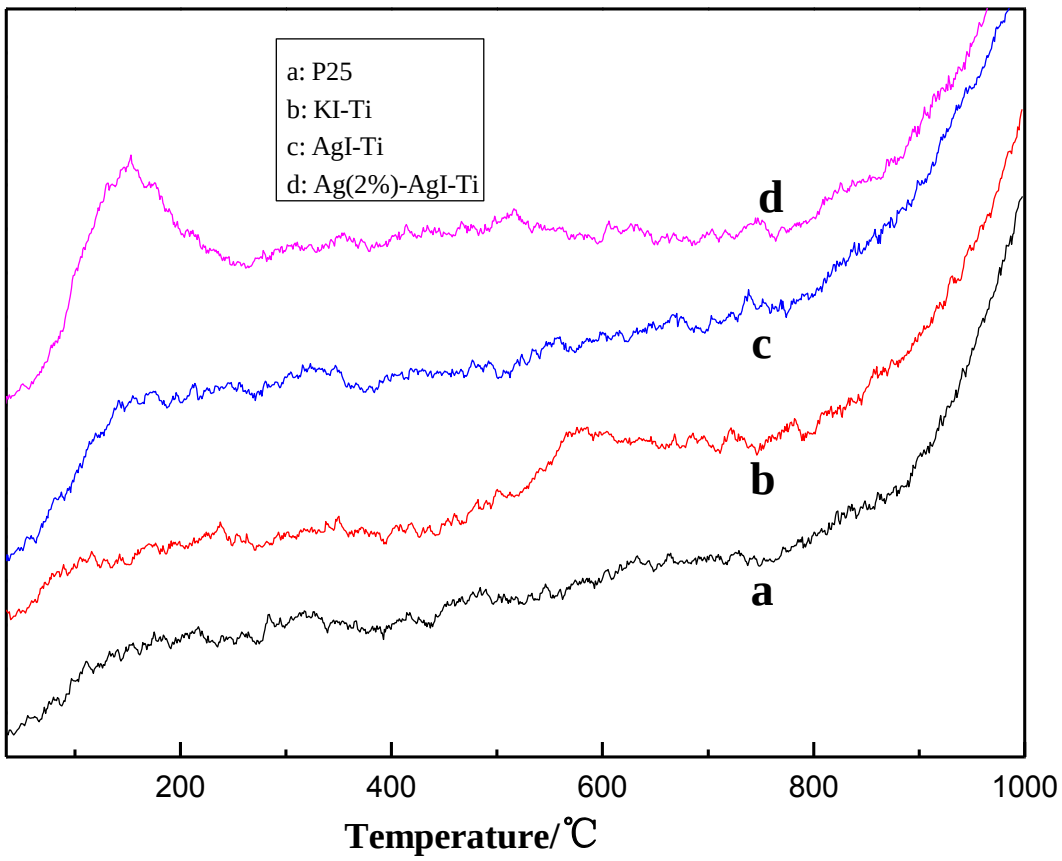

548 **Figure 8**

549

550

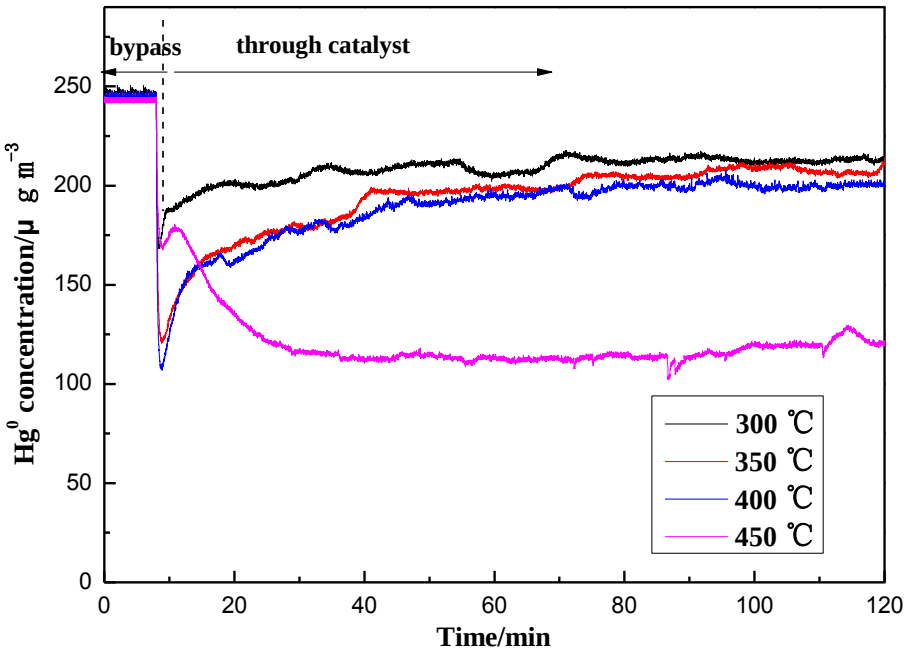

551 **a**

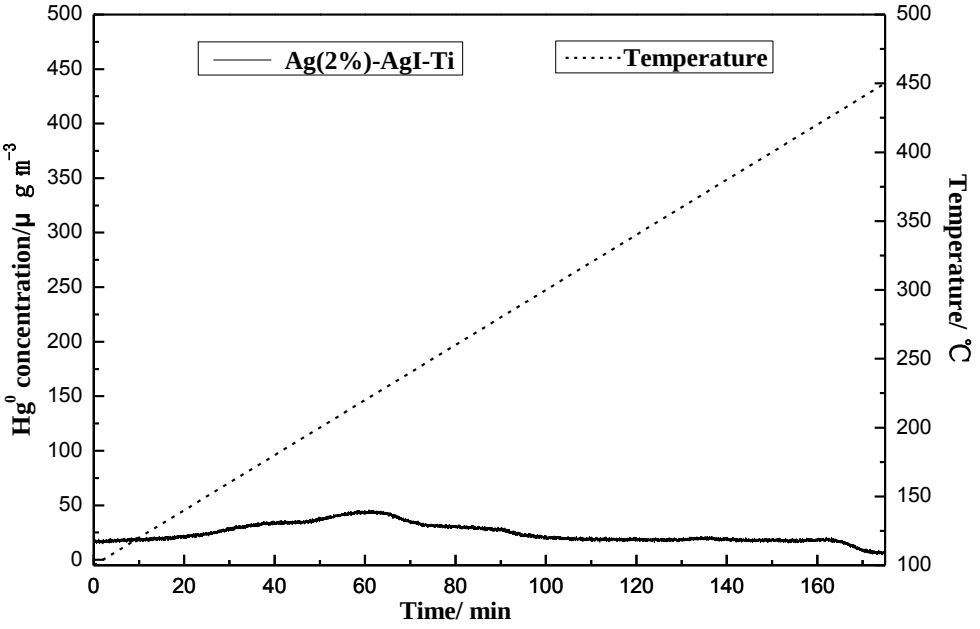

552 **b**

553

554 **Figure 9**

555

556

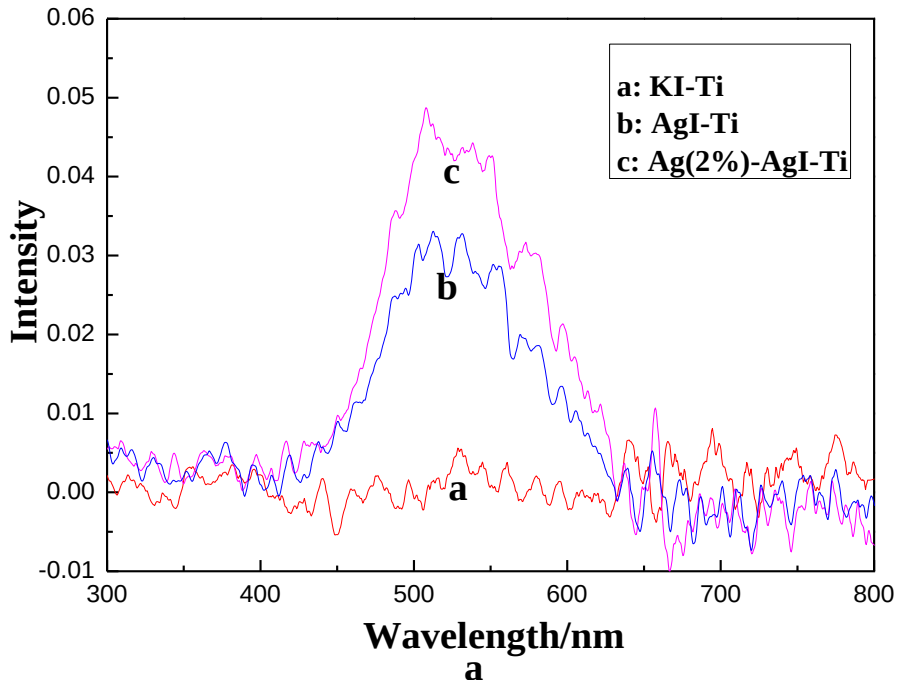

557

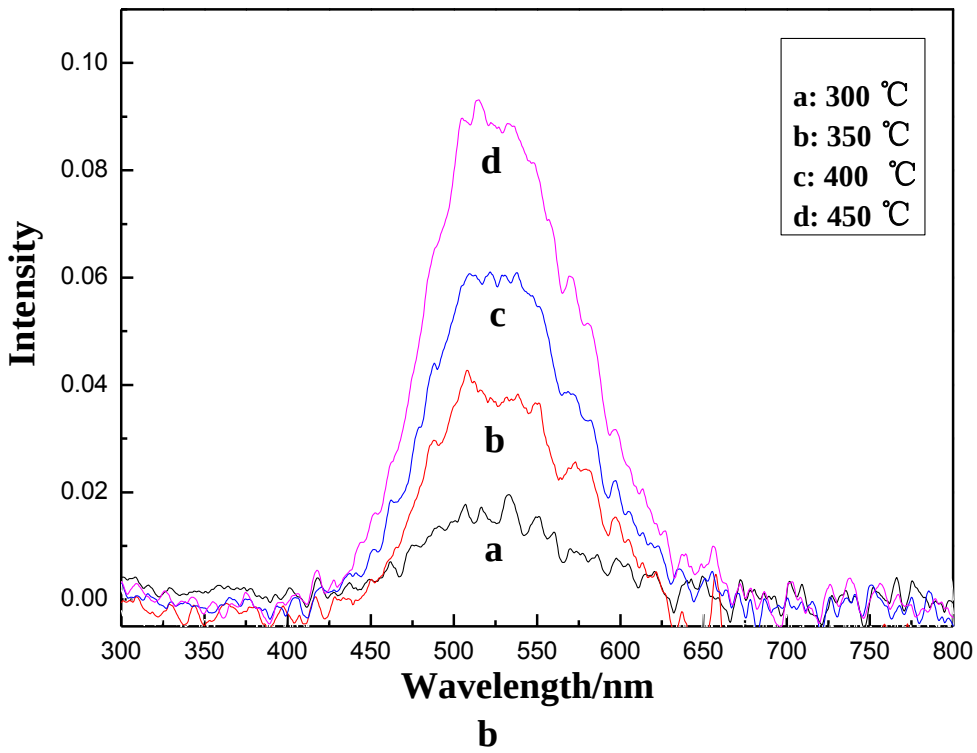

558

559

560

561 **Figure 10**

562

563

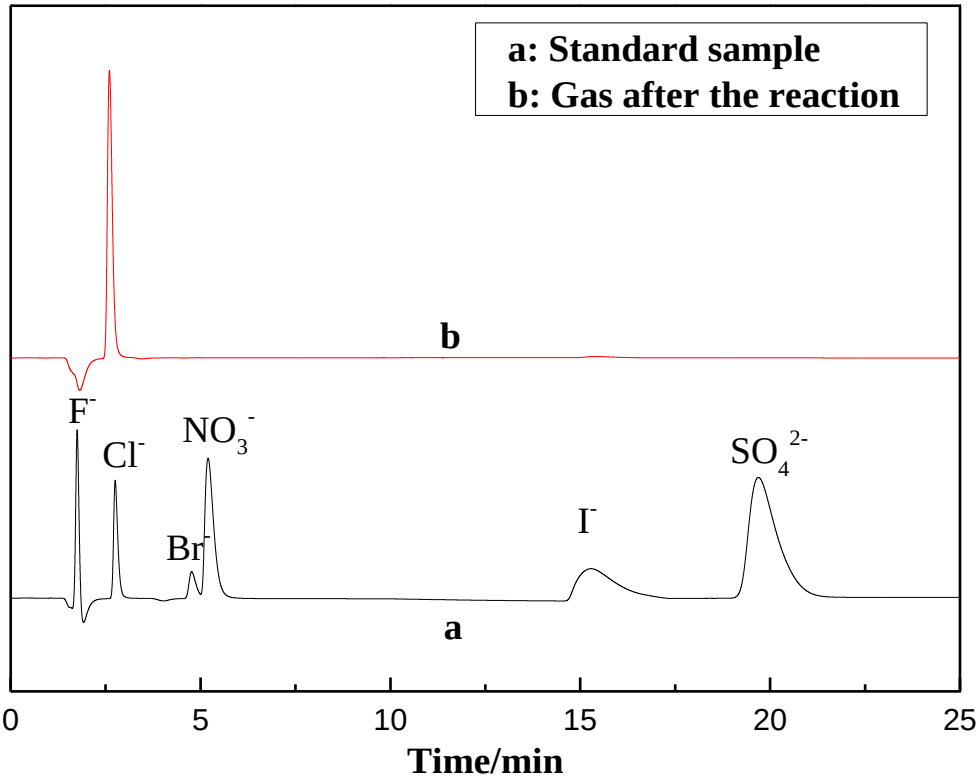

564

565

566 **Figure 11**

567

568

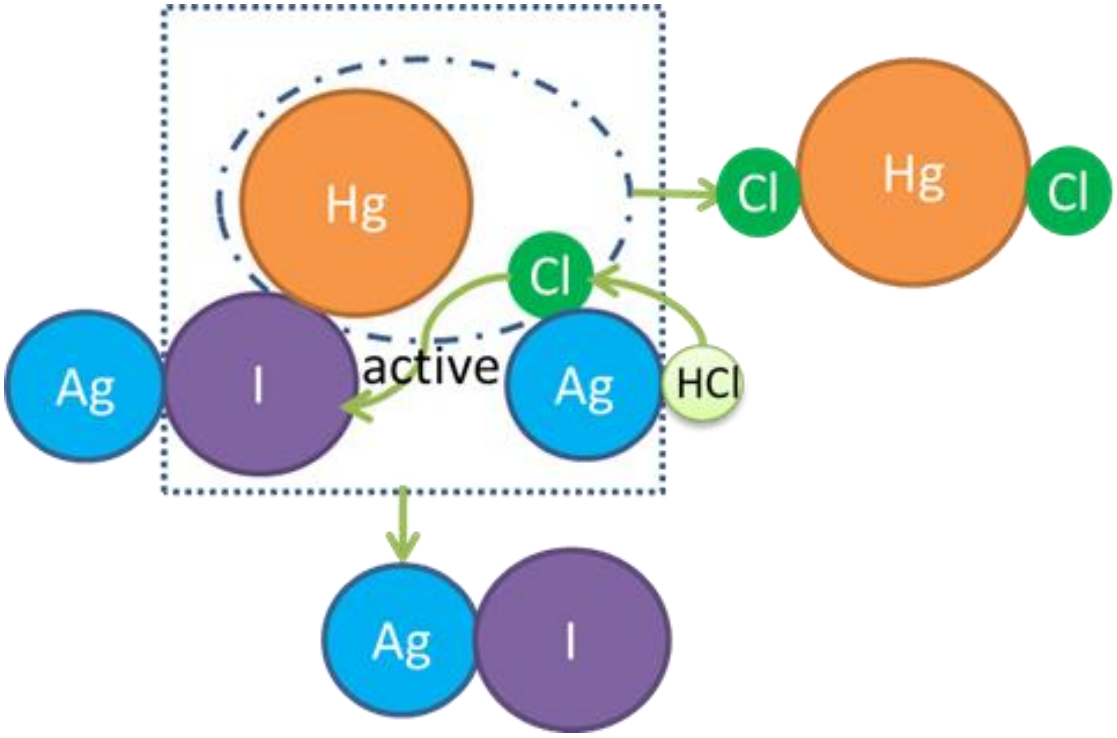

569

570

571 **Figure 12**

572

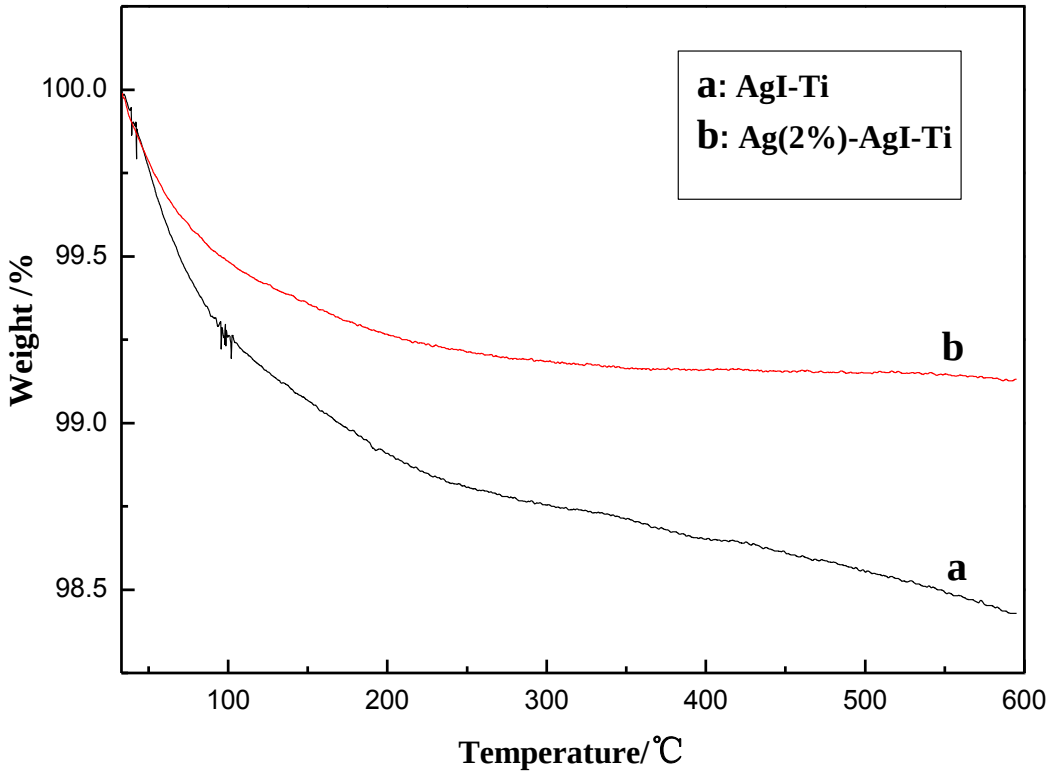

573

574

575 **Figure 13**

576

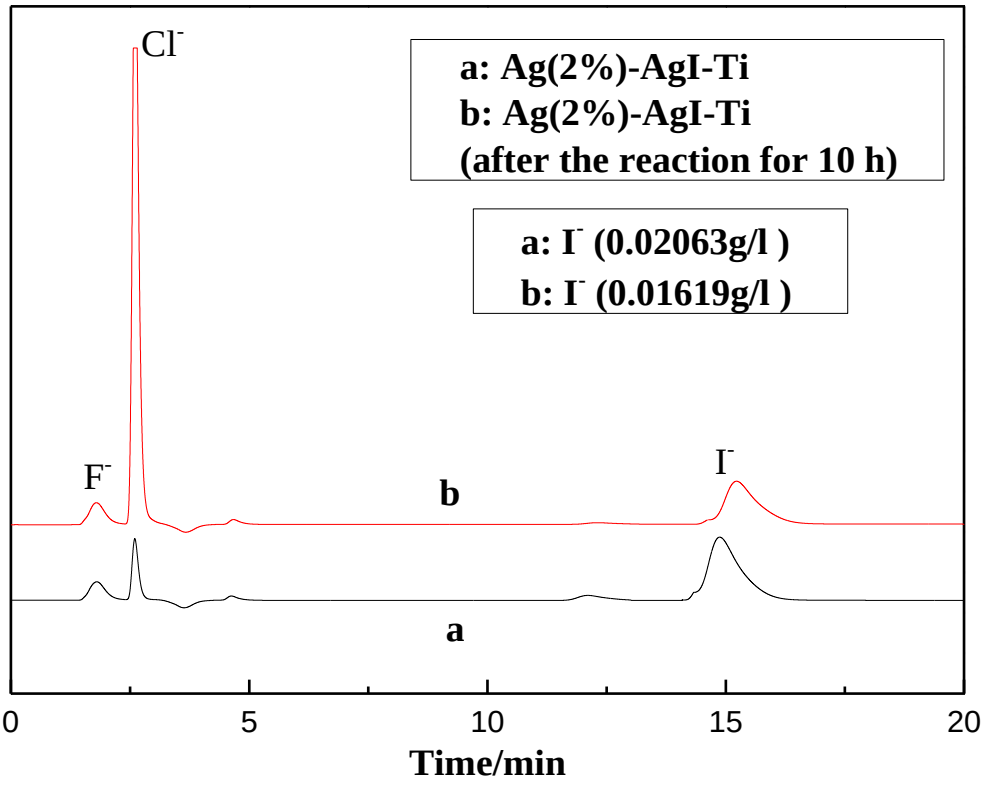

577

578